

# Treatment-Specific Composition of the Gut Microbiota Is Associated With Disease Remission in a Pediatric Crohn's Disease Cohort

Daniel Sprockett, MSc,<sup>\*a</sup> Natalie Fischer, PhD,<sup>†a</sup> Rotem Sigall Boneh, RD,<sup>‡</sup> Dan Turner, MD,<sup>§</sup> Jarek Kierkus, MD, PhD,<sup>¶</sup> Malgorzata Sladek, MD, PhD,<sup>||</sup> Johanna C. Escher, MD, PhD,<sup>\*\*</sup> Eytan Wine, MD, PhD,<sup>††</sup> Baruch Yerushalmi, MD,<sup>‡‡</sup> Jorge Amil Dias, MD,<sup>§§</sup> Ron Shaoul, MD,<sup>¶¶</sup> Michal Kori, MD,<sup>|||</sup> Scott B. Snapper, MD, PhD,<sup>\*\*\*†††</sup> Susan Holmes, PhD,<sup>‡‡‡</sup> Athos Bousvaros, MD,<sup>\*\*\*</sup> Arie Levine, MD,<sup>‡b,§§§</sup> and David A. Relman, MD<sup>\*,†,¶¶¶,b,⊙</sup>

**Background:** The beneficial effects of antibiotics in Crohn's disease (CD) depend in part on the gut microbiota but are inadequately understood. We investigated the impact of metronidazole (MET) and metronidazole plus azithromycin (MET+AZ) on the microbiota in pediatric CD and the use of microbiota features as classifiers or predictors of disease remission.

**Methods:** 16S rRNA-based microbiota profiling was performed on stool samples from 67 patients in a multinational, randomized, controlled, longitudinal, 12-week trial of MET vs MET+AZ in children with mild to moderate CD. Profiles were analyzed together with disease activity, and then used to construct random forest models to classify remission or predict treatment response.

**Results:** Both MET and MET+AZ significantly decreased diversity of the microbiota and caused large treatment-specific shifts in microbiota structure at week 4. Disease remission was associated with a treatment-specific microbiota configuration. Random forest models constructed from microbiota profiles before and during antibiotic treatment with metronidazole accurately classified disease remission in this treatment group (area under the curve [AUC], 0.879; 95% confidence interval, 0.683–0.9877; sensitivity, 0.7778; specificity, 1.000;  $P < 0.001$ ). A random forest model trained on pre-antibiotic microbiota profiles predicted disease remission at week 4 with modest accuracy (AUC, 0.8;  $P = 0.24$ ).

**Conclusions:** MET and MET+AZ antibiotic regimens in pediatric CD lead to distinct gut microbiota structures at remission. It may be possible to classify and predict remission based in part on microbiota profiles, but larger cohorts will be needed to realize this goal.

**Key Words:** pediatric Crohn's disease, microbiota, antibiotics, disease remission, random forest model

Received for publications March 3, 2019; Editorial Decision May 29, 2019.

From the \*Department of Microbiology & Immunology, Stanford University School of Medicine, Stanford, California, USA; †Division of Infectious Diseases & Geographic Medicine, Department of Medicine, Stanford University School of Medicine, Stanford, California, USA; ‡Pediatric Gastroenterology and Nutrition Unit, Wolfson Medical Center, Holon, Israel; §The Juliet Keidan Institute of Pediatric Gastroenterology & Nutrition, Shaare Zedek Medical Center, The Hebrew University of Jerusalem, Jerusalem, Israel; ¶Department of Gastroenterology, Hepatology, Feeding Disorders and Pediatrics, The Children's Memorial Health Institute, Warsaw, Poland; †Department of Pediatrics, Gastroenterology and Nutrition, Jagiellonian University Medical College, Cracow, Poland; \*\*Department of Pediatric Gastroenterology, Erasmus MC-Sophia Children's Hospital, Rotterdam, the Netherlands; ††Division of Pediatric Gastroenterology and Nutrition, Department of Pediatrics, University of Alberta, Edmonton, Canada; ‡‡Pediatric Gastroenterology Unit, Soroka University Medical Center, and Faculty of Health Sciences, Ben-Gurion University of the Negev, Beer Sheva, Israel; §§Department of Pediatrics, Hospital de Sao Joao, Porto, Portugal; ¶¶Pediatric Gastroenterology Unit, Ruth Children's Hospital, Rambam Medical Center, Haifa, Israel; |||Pediatric Day Care Unit, Kaplan Medical Center, Rehovot, Israel; \*\*\*Division of Gastroenterology, Hepatology, and Nutrition, Boston Children's Hospital, Boston, Massachusetts, USA; †††Division of Gastroenterology, Brigham and Women's Hospital, and Harvard Medical School, Boston, Massachusetts, USA; ‡‡‡Department of Statistics, Stanford University, Stanford, California, USA; §§§Sackler School of Medicine, Tel Aviv University, Tel Aviv, Israel; ¶¶¶Infectious Diseases Section, Veterans Affairs Palo Alto Health Care System, Palo Alto, California, USA

Supported by: This research was funded by National Science Foundation Graduate Research Fellowship DGE-114747 (D.S.), National Institute of General Medical Sciences of the National Institutes of Health training grant T32GM007276 (D.S.), The Leona M. and Harry B. Helmsley Charitable Trust grant 2014PG-IBD014 (D.A.R.), the Thomas C. and Joan M. Merigan Endowment at Stanford University (D.A.R.), and the Chan Zuckerberg Biohub Microbiome Initiative (D.A.R.).

Conflicts of interest: R.S.B. has received speaker fees from Nestlé Health Science and Takeda and consulting fees from Nestlé Health Science. D.T. has received consulting fees, research support, royalties, or honoraria from Janssen, Pfizer, Hospital for Sick Children, Ferring, Abbvie, Takeda, Biogen, Atlantic Health, Shire, Celgene, Lilly, Neopharm, and Roche. J.C.E. has received grants from and served on advisory boards for Merck, Janssen, and Abbvie. E.W. has received advisory fees from Abbvie, travel support from Janssen and Abbvie, and speaker fees from Nestlé and Abbvie. R.S. has received travel support from Janssen and Takeda and consulting fees from Abbvie. S.B.S. has received research support from Pfizer, Janssen, Merck, and Regneron, serves on advisory boards for Pfizer, Janssen, IFM Therapeutics, Celgene, Pandion, Applied Molecular Transport, and Eli Lilly, has received consulting fees from Amgen and Hoffman LaRoche, and has received royalties from UpToDate. A.B. has received research support from Prometheus, Janssen, Abbvie, Takeda, and Buhlmann, consulting fees from Shire, Takeda, Best Doctors, Alivio, and Eli Lilly, and royalties from UpToDate. A.L. has received grants from Nestlé Health Science and Janssen and consulting fees from Celgene, Takeda, and Abbvie. D.A.R. has received stock options from ArcBio, Evelo, Karius, NanoBio, ProdermiQ, Second Genome, and Seres Therapeutics and serves on advisory boards for ArcBio and Karius.

Address correspondence to: David A. Relman, MD, VA Palo Alto Health Care System, 154T, 3801 Miranda Avenue, Palo Alto, CA 94304 ([relman@stanford.edu](mailto:relman@stanford.edu)).

<sup>a</sup>Equal contribution

<sup>b</sup>Equal contribution

Published by Oxford University Press on behalf of Crohn's & Colitis Foundation 2019.  
This work is written by (a) US Government employee(s) and is in the public domain in the US.

doi: 10.1093/ibd/izz130

Published online 5 July 2019

## INTRODUCTION

The global incidence of Crohn's disease (CD) has steadily risen over the past few decades, especially among pediatric patients.<sup>1</sup> Early diagnosis and timely and effective personalized treatment are especially crucial in this vulnerable patient population, as the disease in childhood may be more extensive and may follow a more severe course, with children experiencing growth failure or delayed puberty and life-long consequences.<sup>2,3</sup> Efforts are being made to identify novel noninvasive biomarkers in CD patients, not only to monitor disease severity but also to predict therapeutic response.<sup>4,5</sup>

Genome-wide association studies have identified a variety of risk loci within genes important for the maintenance of homeostasis with our commensal gut microbiota.<sup>6</sup> In this regard, several studies in pediatric CD patients have described a state of microbiome "dysbiosis," with varying claims about disease-promoting or -ameliorating bacterial taxa<sup>7-9</sup> and about differences in bacterial diversity.<sup>10</sup> Antibiotics in general have a large effect on the microbiome, but the magnitude of the effect differs among individuals, as do taxa-specific responses to the same antibiotic treatment in different individuals.<sup>11</sup> Similarly, several trials in adult CD have found, in general, a benefit from antibiotic treatment, but with heterogeneous results for the use of metronidazole, quinolones, and rifaximin.<sup>12</sup>

Metronidazole (MET) is one of the most commonly prescribed antibiotics in the treatment of pediatric CD, but recent studies have reported superior outcomes for the combination of MET plus azithromycin (AZ), as compared with MET alone.<sup>13,14</sup> Azithromycin is especially promising in the treatment of inflammatory bowel disease (IBD), as it penetrates multiple intestinal compartments, including the intestinal lumen, biofilms in the mucus layer, and macrophages.<sup>15,16</sup> The use of AZ might improve treatment of various pathogens implicated in CD, such as adherent and invasive *Escherichia coli* (AIEC) strains.<sup>17-19</sup>

The goal of this study was to evaluate the intestinal microbiota as a source of predictors of disease state and of treatment response in pediatric CD patients undergoing either single (MET) or combination (MET+AZ) antibiotic therapy. We took advantage of a randomized controlled trial of those 2 antibiotic regimens in pediatric CD and examined the treatment-specific impact on microbiome diversity and composition; we then employed machine-learning techniques to identify microbiota composition-based signatures associated with antibiotic treatment that might enable monitoring of disease and guide clinical decision-making.

## METHODS

### Study Design

Seventy-four CD patients (aged 5–18 years) were previously enrolled at 11 pediatric gastroenterology clinical

sites in an investigator-blinded randomized controlled trial comparing the efficacy of MET+AZ vs MET therapy for the treatment of children with mild to moderate active CD (10 < Pediatric Crohn's Disease Activity Index [PCDAI] ≤ 40; National Institutes of Health NCT01596894). Sixty-seven of those 74 patients from 9 sites provided stool samples for the microbiome study reported here. A complete description of the study design, laboratory and analysis methods, and primary outcomes has been published previously.<sup>13</sup> Additional inclusion criteria, besides age and disease activity, included at least 1 elevated inflammatory marker above normal values (C-reactive protein [CRP], erythrocyte sedimentation rate [ESR], or calprotectin) and disease duration since diagnosis <3 years. Exclusion criteria included presence of a stool pathogen (based on bacterial culture, parasite study, or *Clostridium difficile* toxin assay), involvement of the proximal ileum or jejunum (L4b, as per Paris classification), unclassified IBD, fibrostenotic disease (defined as strictures with prestenotic dilatation), internal or perianal fistulizing disease, prominent extraintestinal manifestations (eg, arthritis, uveitis, and sclerosing cholangitis), known allergy to either metronidazole or azithromycin, prolonged QT<sub>c</sub> at baseline, or steroid use during the 7 days before enrollment.

The treatment protocol was adapted from a report by Levine and Turner.<sup>14</sup> Patients were enrolled in 1 of the 2 treatment arms with 1:1 randomization, although 11 subjects with a lack of response to MET therapy received open-label AZ between weeks 4 and 8. These MET/MET+AZ subjects were treated as a separate group for analyses involving time points after week 4. Furthermore, 4 patients in the MET group, 5 patients in the MET+AZ group, and 1 patient in the MET/MET+AZ group received steroids or biologics after week 4 at their physician's direction due to inadequate response. Both the MET and MET+AZ groups discontinued antibiotics after week 8, whereas the MET/MET+AZ group maintained their regimen to complete a total of 8 weeks. Sixty-seven patients participated in the microbiome study, where stool samples for microbiota analysis were collected at weeks 0, 4, 8, and 12. Disease activity was determined using the PCDAI, and clinical remission was defined as a PCDAI <10.

### Study Procedures for Assessment of Inflammatory Markers

A blood sample for measurement of CRP, ESR, complete blood count, and serum albumin was collected at each visit, and a fecal sample for measurement of calprotectin was collected at weeks 0 and 8. Stool extracts were prepared using the BÜHLMANN Smart-Prep kit (Buhlmann Laboratories AG, Schönenbuch, Switzerland). Fecal calprotectin was measured using the fCAL enzyme-linked immunosorbent kit (Buhlmann Laboratories AG, Schönenbuch, Switzerland) with a normal range <100 µg/g. Preliminary results indicated very high levels of fecal

calprotectin (>1800 µg/g) in many patients; therefore, all samples were diluted 1:10 according to the manufacturer's instructions.

## Microbiota Analysis

Stool samples were collected and frozen on site at -20°C and then shipped to a central laboratory and stored at -80°C until further processing. DNA was extracted from ~200 mg of stool using the QIAGEN DNeasy PowerSoil HTP 96 Kit (Qiagen, Germantown, MD, Cat #12955-4) following the manufacturer's instructions, including a 2×10-minute bead-beating step using the Retsch 96 Well Plate Shaker at speed 20. The V4 region of the 16S rRNA gene was amplified using forward primer 515F (5'-GTGCCAGCAGCCGCGGTAA-3') with an error-correcting barcode and 806R (5'-GGACTACAGGGTATCTAAT-3').<sup>20</sup> Polymerase chain reaction products were then purified, pooled in equimolar concentrations, and sequenced on three 2×300 Illumina MiSeq paired-end runs using the reagent kit, version 3.

Raw reads were demultiplexed using the QIIME command `split_libraries_fastq.py` (QIIME, version 1.9.1) and then quality-trimmed using the DADA2 pipeline (`dada2`, version 1.1.1) in R (R, version 3.2.4).<sup>21</sup> Briefly, forward reads were truncated to 220 bp, and reverse reads to 150 bp, and quality-filtered with the following settings: `maxN = 0`, `maxEE = 2`, `truncQ = 2`. After quality trimming, amplicon sequence variants (ASVs) were inferred using the DADA2 pipeline. Taxonomy was assigned to each ASV using the RDP classifier and the SILVA 16S rRNA database (SILVA nr, version 132), and a phylogenetic tree was built from the ASVs using the `phangorn` R package (`phangorn`, version 2.4.0). The ASV table, patient sample data, taxonomy assignments, phylogenetic tree, and ASV sequences were then bundled into a single `phyloseq` data object for further plotting and statistical analysis (`phyloseq`, version 1.24.2).<sup>22</sup> Faith's Phylogenetic Diversity was calculated using the R package `picante` (`picante`, version 1.7), and distance calculations and ordination plots were built using the `phyloseq` package. Hierarchical clustering of ASVs was performed using the `hclust` function in the `stats` R package (`stats`, version 3.5.1). Differential abundance tests were carried out using the `DESeq2` R package (`DESeq2`, version 1.20.0). Analysis of variance in the data set was assessed with permutational analysis of variance (PERMANOVA) (`vegan`, version 2.5–4) with 1000 permutations on the Unifrac distance matrix. Bonferroni correction was applied for multiple comparisons (`p.adjust` function in the `stats` package, version 3.5.1).

## Random Forest Modeling

Machine learning analyses were performed using the `caret` and `randomForest` R packages (`caret`, version 6.0.80; `randomForest`, version 4.6.14). Before model building, the ASV abundance was transformed using a variance-stabilizing transformation to normalize for sequencing depth in the `DESeq2` R package and centered to reduce the influence of interindividual variation. Models were constructed with samples from subjects

in the MET group only. Model 1 was constructed on microbiota data from weeks 4 and 8, and Model 2 was constructed on microbiota data from weeks 0, 4, and 8, with the outcome variable being disease state (ie, remission or nonremission) at the time of sample collection. Each model was trained on samples from a random subset of 70% of subjects, with generation of 1000 trees and leave-one-out cross-validation. To assess their accuracy, models were used to predict remission or nonremission in samples from the remaining 30% of subjects. Both sets of classification results were then evaluated by calculating their area under the curve (AUC), as derived from a receiver operating characteristic (ROC) curve analysis using the R package `ROCR` (`ROCR`, version 1.0.7). Each model also calculated importance scores for ASVs based on the increase in prediction error when the ASV in question was left out of the training set via random permutation. Because the numbers of remission and nonremission samples in the MET+AZ group were too uneven to be able to construct a useful model, we focused on the MET group only.

A random forest model was constructed on all pre-antibiotic (week 0) microbiota data and on clinical data, including sex, age, disease duration, tissue involvement (Paris classification<sup>23</sup>), baseline immunomodulators, and baseline CRP and PCDAI, to predict disease state (remission or nonremission) at week 4 in both treatment groups combined. To increase the number of shared features found across samples and decrease the noise among closely related bacterial taxa, ASVs were agglomerated based on their cophenetic distance in the phylogenetic tree at the `h = 0.3` level. These numbered ASV clusters were also labeled by the number of ASVs in the cluster and the genus that was assigned to the majority of the ASVs within the cluster. If >50% of the ASVs within a cluster were not assigned to a single genus, the same majority rule was used iteratively at higher taxonomic levels. Models were constructed and tested as described above. Abundances were normalized using variance-stabilizing transformation (the `vst` function in the `DESeq2` package, version 1.20.0).

Amplicon sequencing data are available at SRA (SRP160897). A detailed description of this analysis, along with all analysis code and raw data used to go from sequences to final figures, is available at the Stanford Digital Repository (<https://purl.stanford.edu/mp935wb0227>) and in the Supplementary Data.

## Ethical Considerations

All patients provided written informed consent, or assent when required, before participation. The study was conducted according to the principles of the Declaration of Helsinki.

## RESULTS

### Clinical Outcomes

A total of 67 patients from 9 sites provided stool samples for microbiome analysis and are included in the present study (Table 1).

Of this group, 36 patients were randomly assigned to receive MET, and 31 to receive MET+AZ (Fig. 1A). Figure 1B shows the temporal dynamics of each patient's PCDAI, measured at the time of stool sample collection (Fig. 1B). By week 4, 42% (15/36) of MET patients and 65% (20/31) of MET+AZ patients had achieved remission (Fig. 1B). Between weeks 4 and 8, 11 of the MET patients failing remission had azithromycin added to their treatment regimen (MET/MET+AZ). At week 8, 60% (15/25) of patients in the remaining MET group, 65% (20/31) in the MET+AZ group, and 45% (5/11) in the new MET/MET+AZ group had achieved remission. At week 12, 72% (18/25) of the individuals in the remaining MET group were in remission, whereas 71% (22/31) of the MET+AZ group and 100% (11/11) of the MET/MET+AZ group were in remission. Differences in remission rates and inflammatory markers between the data presented here (per protocol analysis) and the original clinical paper<sup>13</sup> (intention-to-treat analysis) are due to the transfer of treatment failures out of the MET group to the MET/MET+AZ group, thus reducing the number of inflamed nonresponders in the MET group.

Of note, our analysis included samples from 2 patients in the MET group and 2 patients in the MET+AZ group who did not respond to antibiotic treatment by week 4 and either received open-label steroids at week 4 or biologics at week 8. In addition, 6 patients in the MET group, 7 patients in the MET+AZ group, and 3 patients in the MET/MET+AZ group received additional immunomodulators at some point during the study. Accordingly, not all clinical improvement in these patients could necessarily be attributed to the antibiotic regimen alone. Therefore, we examined the effect of additional drugs on achievement of remission. There was no difference between

patients who started at baseline on either aminosalicylates (chi-square test,  $P = 0.43$ ) or immunomodulators (chi-square,  $P = 0.10$ ). Patients who received additional immunomodulators during the study were less likely to achieve remission (chi-square test,  $P < 0.01$ ). There was no difference between the numbers of patients who achieved remission after addition of steroids or biologics during the study and the numbers of patients achieving remission without additional drugs (chi-square test: steroids  $P = 0.55$ ; biologics  $P = 0.35$ ).

Calprotectin, CRP, and ESR are prominent markers of inflammation, currently measured in the clinic and interpreted by health care providers to determine disease status. CRP values decreased significantly in all 3 groups from weeks 0 to 4 of treatment (Wilcoxon test, MET  $P = 0.0046$ ; MET+AZ  $P = 3.2e-05$ ; MET/MET+AZ  $P = 0.023$ ), with no further significant changes from weeks 4 to 8 (Supplementary Fig. 1A). Fecal calprotectin was generally high (>1800 ug/g) at weeks 0 and 8 and decreased significantly in the MET+AZ (Wilcoxon test,  $P = 0.0093$ ) and the MET/MET+AZ groups (Wilcoxon test,  $P = 0.0074$ ), but not in the MET group (Supplementary Fig. 1B). We did not observe any significant changes in ESR levels after antibiotic treatment in any of the 3 groups (Wilcoxon test,  $P \leq 0.05$ ), indicating that ESR might not be a good readout of disease status in this patient cohort (Supplementary Fig. 1C).

## Microbiota Response to Single and Combination Antibiotic Therapies

Antibiotics can strongly perturb the distal gut microbiota in an individual-specific manner<sup>24</sup>; individualized

**TABLE 1.** Study Subject Features at Baseline

	MET Group	MET+AZ Group
Subjects	36	31
Samples	120	112
Female/male	20/16	6/25
Age, mean $\pm$ SD, y	13.5 $\pm$ 3.1	14.2 $\pm$ 3.1
Disease duration, mean $\pm$ SD, y	0.7 $\pm$ 1	1.1 $\pm$ 1.1
Baseline PCDAI $\pm$ SD	19.6 $\pm$ 8.1	22 $\pm$ 9
Disease location (Paris classification)		
L1	13	6
L2	1	2
L3	22	23
L4a	18	16
Treatment at baseline		
Immunomodulators	14	19
Aminosalicylates	6	11
Antibiotics within the previous 12 mo	2	2

Sixty-seven pediatric Crohn's disease patients were randomly assigned to treatment with either metronidazole or metronidazole plus azithromycin. Sex (chi-square test,  $P < 0.01$ ) and number of subjects with L1 involvement (chi-square test,  $P < 0.01$ ) differed significantly between the 2 groups.

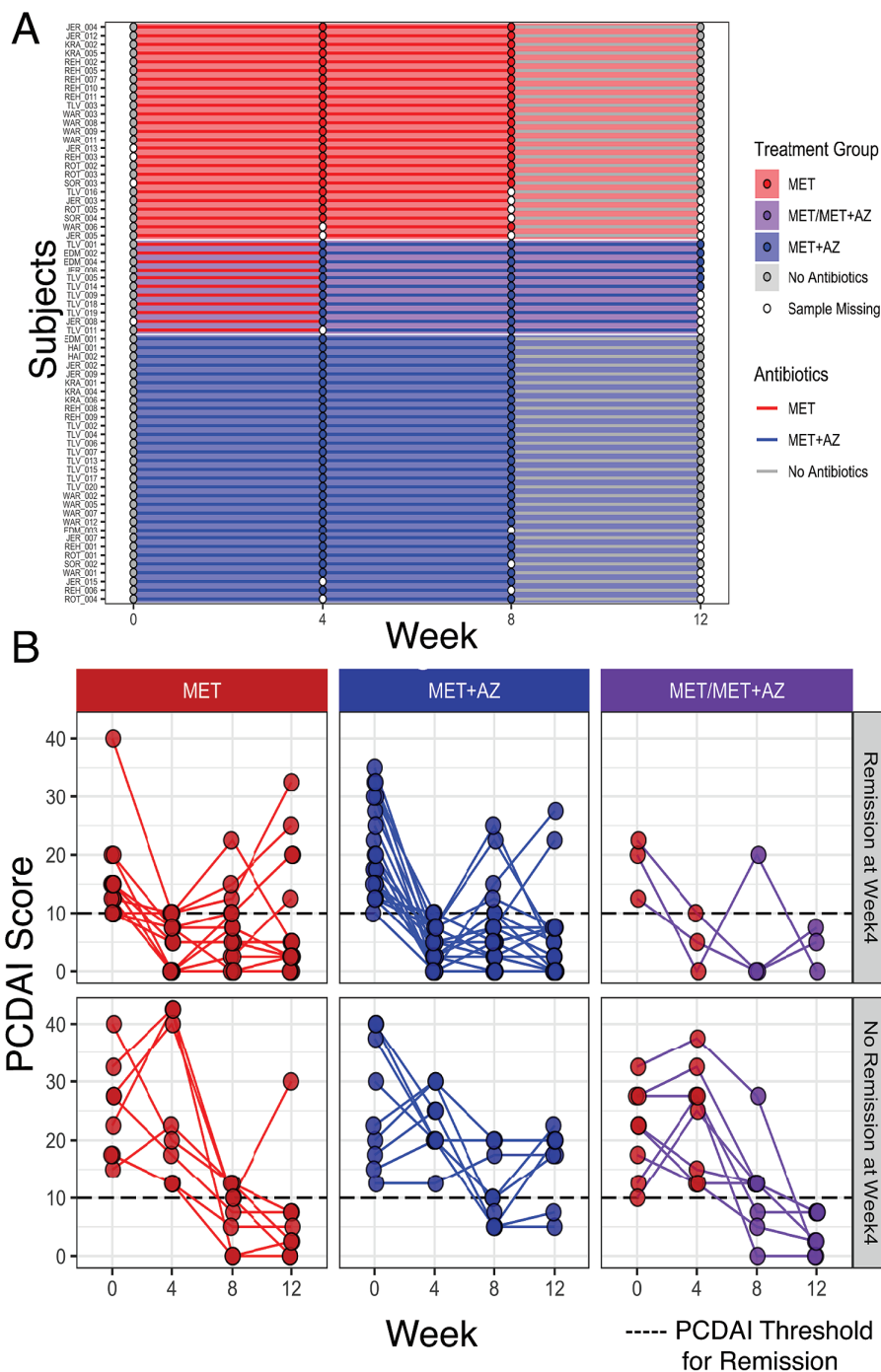


FIGURE 1. Study design and clinical outcomes. A, At week 0, 67 pediatric Crohn's disease patients were randomly assigned to 1 of 2 treatment groups: MET subjects (n = 36, red) received 20 mg/kg metronidazole twice daily (maximum of 1000 mg/d) for 8 weeks, whereas MET+AZ subjects (n = 31, blue) received metronidazole plus 7.5 mg/kg of azithromycin (maximum of 500 mg/d) once a day for 5 consecutive days, followed by a 2-day drug holiday, each week for the first 4 weeks and then stepped down to 3 consecutive days of the same dose with a 4-day drug holiday per week over the subsequent 4 weeks. Patients not in remission between weeks 4 and 8 could be offered open-label azithromycin based on physician assessment (purple, n = 11); they are displayed as a distinct patient cohort from weeks 4 to 12. Stool samples were collected at weeks 0, 4, 8, and 12. B, Pediatric Crohn's Disease Activity Index for subjects at weeks 0, 4, 8, and 12. Treatment groups (MET, red; MET+AZ, blue; MET/MET+AZ, purple) are in columns, whereas the rows are groups of subjects who were either in remission (top) or not in remission (bottom) at week 4.

responses might explain some of the observed heterogeneity in disease progression and dynamics. First, we characterized the microbiome of all patients at baseline. We calculated the mean Faith's phylogenetic diversity and observed no differences between the 3 treatment groups at baseline (Supplementary Fig. 2A). Next, we calculated the mean unweighted UniFrac pairwise distance among all samples and did not observe significant differences in microbiome composition between the treatment groups at baseline (PERMANOVA, corrected

$P = 1$ ) (Supplementary Fig. 2B). As sex and number of subjects with L1 Paris classification were unequally distributed between the MET and MET+AZ groups at baseline, we also tested for the potential influence of these factors on baseline microbiome composition and detected no difference between male and female patients (PERMANOVA, corrected  $P = 1$ ) (Supplementary Fig. 2C) or by L1 Paris classification status (PERMANOVA, corrected  $P = 0.25$ ) (Supplementary Fig. 2D). Patients with baseline use of immunomodulators or

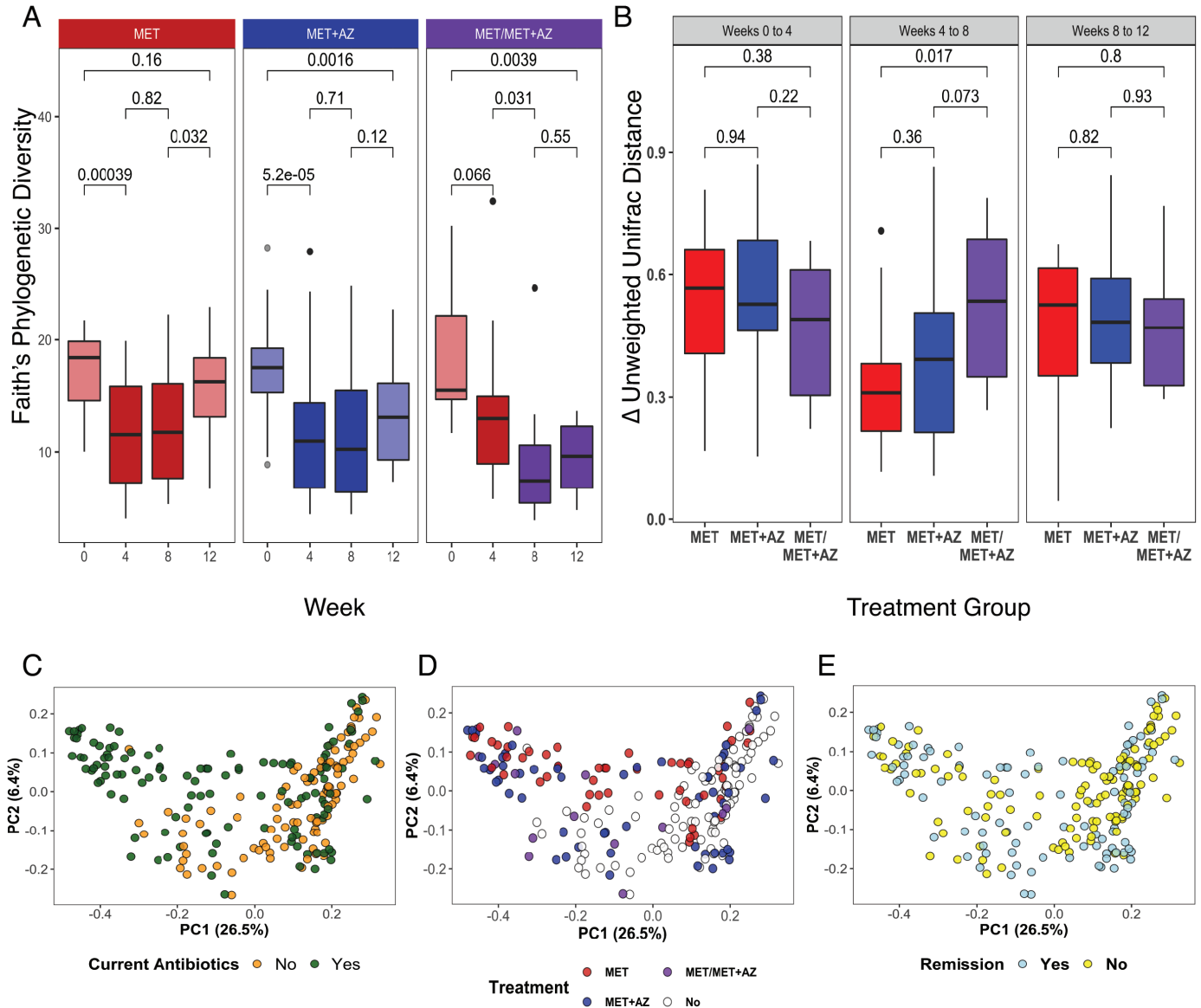


FIGURE 2. Microbiota response to antibiotic therapy. A, Alpha diversity measured by Faith's Phylogenetic Diversity, segregated by treatment group (MET, red; MET+AZ, blue; MET/MET+AZ, purple) and week. Treatment group colors are darker during antibiotic treatment.  $P$  values are displayed for comparisons between treatments (Wilcoxon test). B, Boxplot of the median intrasubject unweighted UniFrac pairwise distance among samples collected during consecutive time points. C–E, Principal coordinates analysis on the unweighted UniFrac pairwise distances among all samples and all subjects. Samples are colored by (C), current antibiotic use, yes/no (PERMANOVA,  $P < 0.01$ ); (D) current antibiotic use and treatment group (PERMANOVA,  $P = 0.1$ ) and remission status (PERMANOVA,  $P < 0.05$ ); and (E) current disease state, in remission or not. The significance of treatment group clustering was determined by PERMANOVA (adonis) with 1000 permutations. Bonferroni correction was applied for multiple comparisons.

aminosalicylates had a stable disease state at the start of the study and were not excluded; they continued their medication throughout.

Aminosalicylates had a significant impact on baseline microbiome composition (PERMANOVA, corrected  $P < 0.05$ ) (Supplementary Fig. 2E), but immunomodulators had no impact on baseline microbiome composition (PERMANOVA, corrected  $P = 0.13$ ) (Supplementary Fig. 2F). As the distribution of patients receiving 5ASA was similar in each of the treatment groups, we did not exclude those patients from the analysis.

We observed a profound shift in gut microbiota diversity and structure after antibiotic administration in most subjects. In the MET and MET+AZ treatment groups, alpha diversity decreased significantly (Wilcoxon test,  $P \leq 0.01$ ) (Fig. 2A). Diversity remained low in both groups at week 8 and rebounded toward its pre-antibiotic level by week 12, after discontinuation of antibiotics. Yet, only the MET group achieved a level of diversity that was comparable to its baseline state (Wilcoxon test, MET week 0 vs 12  $P = 0.16$ ), whereas the MET+AZ group's mean diversity remained significantly lower (Wilcoxon test, MET+AZ week 0 vs 12  $P \leq 0.01$ ).

Subjects in the MET group who were subsequently given AZ (MET/MET+AZ) after week 4 experienced a nonsignificant decrease in mean diversity at week 4 (Wilcoxon test, week 0 vs week 4  $P = 0.07$ ), consistent with this subgroup's initial unresponsiveness to MET. However, after the addition of azithromycin at week 8, the mean diversity decreased significantly (Wilcoxon test, week 4 vs 8  $P \leq 0.05$ ) and became comparable to the level of the MET+AZ group at week 4 (Wilcoxon test,  $P = 0.2$ ). Diversity remained low at week 12 in the MET/MET+AZ group, possibly because many subjects were still receiving their 8-week combination antibiotic regimen at that time.

Next, we examined the magnitude of the change in microbiota structure in response to antibiotics within each treatment group by calculating the median difference in unweighted UniFrac pairwise distance among samples from the same patient at different study time points. The microbiome composition in all 3 treatment groups changed to the same degree between weeks 0 and 4, reflected in a mean unweighted UniFrac pairwise distance of  $\sim 0.5$ , with no significant difference between groups (Fig. 2B). Thereafter, smaller changes occurred between weeks 4 and 8, but the MET/MET+AZ group showed a significantly larger shift in community structure than the MET group, possibly reflecting the addition of azithromycin (Fig. 2B).

We then assessed the contribution of current antibiotic use, treatment group, and remission status to variation in the data using principal coordinates analysis (PCoA) based on unweighted UniFrac distances.<sup>25</sup> The use of antibiotics at the time of sample collection was a significant source of variation (PERMANOVA, corrected  $P < 0.01$ ) (Fig. 2C), as was treatment group (PERMANOVA, corrected  $P < 0.05$ ) (Fig. 2D) and

**TABLE 2.** Impact of Treatment, Disease, and Sex on Microbiome Composition

Variable	$P$	Adjusted $P$ (Bonferroni correction)
Antibiotics	0.000999	0.00999
Treatment group	0.001998	0.01998
Remission	0.002997	0.02997
Sex	0.07193	0.71930
Immunomodulators	0.01598	0.15980
Aminosalicylates	0.008991	0.08991
Steroids	0.1568	1.00000
Infliximab	0.5864	1.00000
EEN	0.1359	1.00000
CDED	0.3307	1.00000

Impact was determined using principal coordinates analysis of the unweighted UniFrac pairwise distances for all samples and all subjects. Analysis of variance in the data set was assessed with PERMANOVA (adonis) with 1000 permutations on the UniFrac distance matrix. Bonferroni correction was applied to adjust for multiple comparisons.

Abbreviations: CDED, Crohn's disease exclusion diet; EEN, exclusive enteral nutrition.

remission status (PERMANOVA, corrected  $P < 0.05$ ) (Fig. 2E). Other variables, such as sex, additional medications, or dietary regimes had no significant impact on the microbiome composition (Table 2; Supplementary Fig. 3).

To identify groups of bacterial taxa with distinct responses to the different antibiotic regimens, we performed differential abundance testing between samples from weeks 0 and 4. ASVs with significant changes in abundance are summarized in a heat map, showing their relative abundance in each treatment group across all time points (Fig. 3). The top 3 clusters of the heatmap show ASVs that increased in abundance during the period of treatment and then decreased after antibiotics were withdrawn. Although ASVs 7 and 61 (both *Enterococcus*) increased in abundance in both treatment groups, ASV 29 (*Streptococcus*) and ASV 27 (*Klebsiella*) increased in the MET group only. This can be explained by the known sensitivity of streptococci and *Klebsiella* to azithromycin and their insensitivity to metronidazole.<sup>26</sup>

ASVs 18 and 2 (both *Bifidobacterium*) and ASV 4 (*Escherichia/Shigella*) increased in abundance in the MET group but decreased in the MET+AZ group. The bottom 3 clusters of the heatmap include ASVs that decreased in abundance during single and/or combination antibiotic treatment and recovered at least partially after cessation of antibiotic administration (Fig. 3). ASVs 10 (*Bacteroides vulgatus*), 114 (*Lachnospiraceae*), 119 (*Lachnoclostridium*), 130 (*Alistipes*), 3 (*Faecalibacterium prausnitzii*), 34 (*Blautia faecis*), 46 (*Alistipes putredinis*), 55 (*Bacteroides caccae*), 57 (*Bacteroides*), 64 (*Terrisporobacter*), 65 (*Coprococcus*), 74 (*Veillonella*), and 97 (*Dorea formicigenerans*) significantly decreased in abundance in the MET treatment group, whereas ASVs 103

(*Morganella morganii*), 165 (*Parabacteroides distasonis*), 17 (*Haemophilus*), 22 (*Bacteroides*), 25 (*Faecalibacterium*), 268 (*Sutterella*), 35 (*Erysipelatoclostridium ramosum*), 38 (*Bacteroides uniformis*), 50 (*Lachnospiraceae*), and 86 (*Ruminococcaceae*) decreased significantly in the MET+AZ group.

### Microbiota and Crohn’s Disease Remission

To understand better how antibiotics might influence microbiota structure and remission, we calculated pairwise Bray-Curtis dissimilarity scores for remission samples and compared those with the pairwise scores for nonremission samples in each treatment group. Week 4 and 8 samples from patients in the MET group who were in remission at that time were significantly more similar to each other than they were to week 4 and 8 samples from patients who were not in remission at the time (Wilcoxon test,  $P \leq 0.001$ ) (Fig. 4A). We observed no significant differences for samples from the MET+AZ group. Furthermore, we found that remission samples from weeks 4 and 8 formed distinct clusters reflecting treatment group (PERMANOVA,

$P \leq 0.001$ ), a finding that was not observed with nonremission samples (PERMANOVA,  $P = 0.1848$ ) (Fig. 4B).

Based on these observations, we sought to identify treatment-specific microbial indicators of CD remission. We used random forest modeling to predict whether a patient was in remission based on their microbiota structure at that time. First, we constructed a model based on the abundances of ASVs found in remission and nonremission samples collected during antibiotic treatment (Model 1, weeks 4 and 8). Because the numbers of remission and nonremission samples in the MET+AZ group were too uneven to be able to construct a useful model, we focused on the MET group only. This model classified remission in the MET patients with an AUC of 0.777 (95% confidence interval [CI], 0.3229–0.8366; sensitivity, 0.8750; specificity, 0.2857;  $P = 0.4006$ ) and classified remission in the MET+AZ group with an AUC of 0.68 (95% CI, 0.4066–0.6764; sensitivity, 0.3846; specificity, 0.8889;  $P = 0.9909$ ) (Fig. 5A) but did not achieve statistical significance in either case. To test an alternative model that incorporated a greater number of nonremission samples, we constructed Model 2 with samples from week 0 as well; these samples represent an alternative

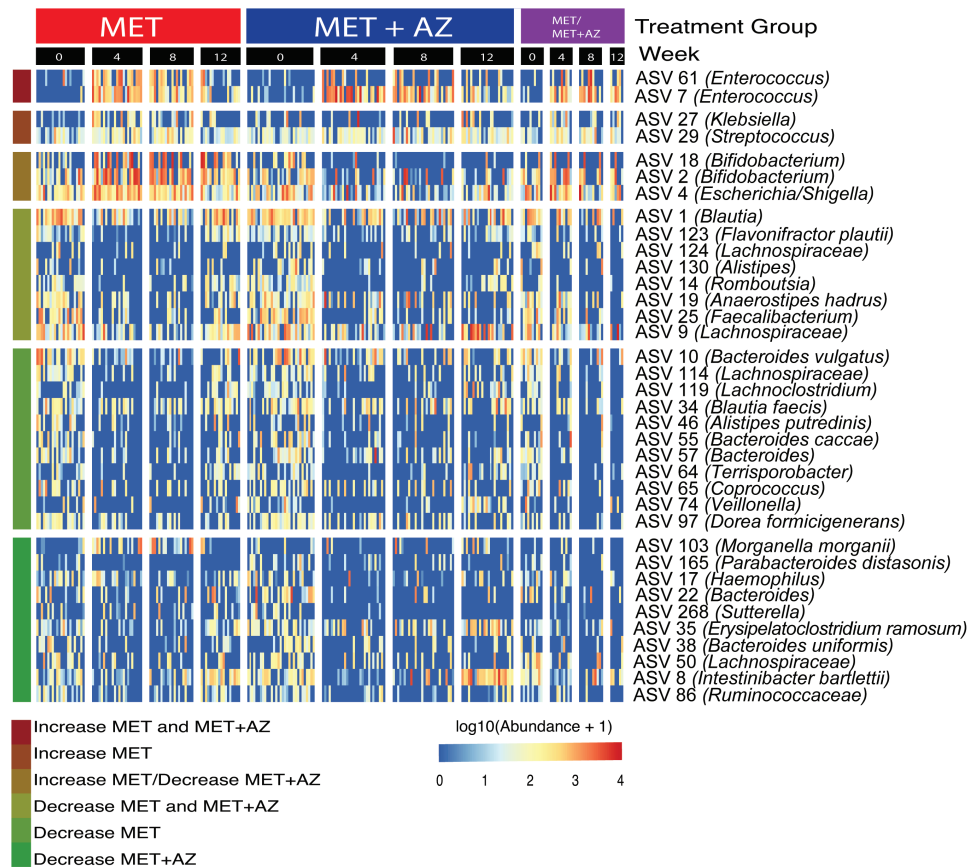


FIGURE 3. Microbial abundances shift in response to antibiotic exposure. ASVs were filtered for presence in at least 20% of samples. Testing for significant differences in ASV abundance between weeks 0 and 4 was performed using DeSeq2 in either the MET or MET+AZ treatment group. Only ASVs with significant differences in abundance between weeks 0 and 4 are displayed. Abundances of ASVs were log<sub>10</sub>-transformed before plotting and partitioned by treatment group and week. Colored bars at the left end of the heatmap denote ASV responses to the treatments.



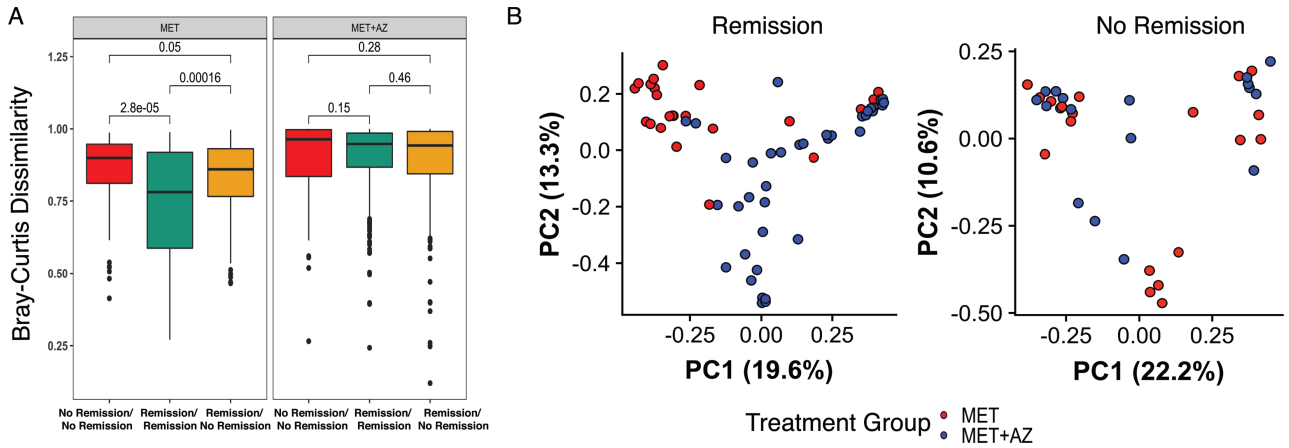


FIGURE 4. Microbiota at time of remission reflects antibiotic exposure. A, Beta-diversity measured by Bray-Curtis dissimilarity between samples in remission and not in remission among MET and MET+AZ subjects during antibiotic treatment (weeks 4 and 8). B, PCoA on the Bray-Curtis dissimilarity of stool samples collected during antibiotic treatment (weeks 4 and 8). The significance of treatment group clustering was determined by PERMANOVA (adonis) with 1000 permutations.

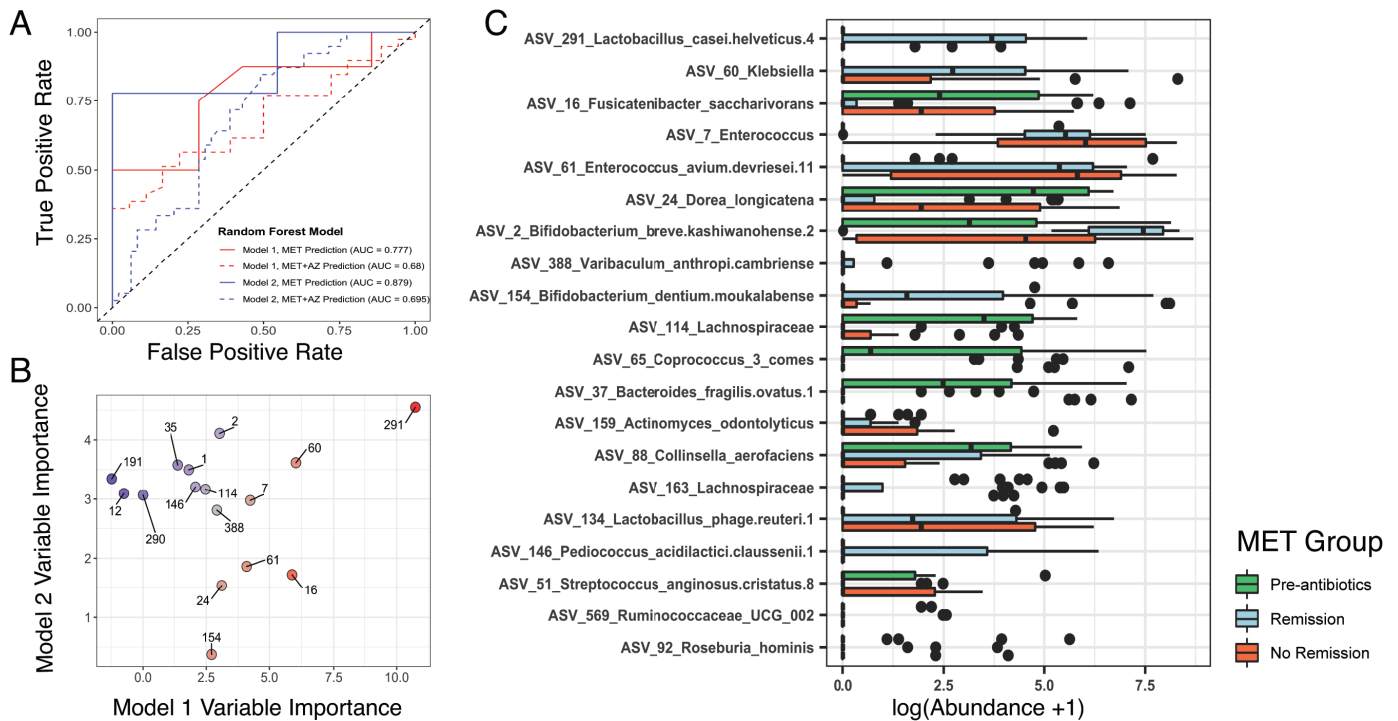


FIGURE 5. Random forest models classify disease remission from microbiota profiles. A, The ROC curves indicate the accuracy of the random forest classification models built using microbiota data. The color of the lines indicates the data set on which the model was trained (Model 1, MET weeks 4 and 8, red; Model 2, MET weeks 0, 4, and 8, blue). Solid lines indicate the accuracy of the model in classifying remission in patients from the same treatment group (MET), whereas the dashed lines indicate the accuracy of each model for classifying remission in patients from the MET+AZ treatment group. B, Variable importance values for the 10 most important ASVs used to build each random forest model are plotted against each other. Points are labeled by ASV number. The point color indicates the importance score (Model 1 specific, red; Model 2 specific, blue; both models, gray). C, Log-transformed abundances of the top 20 ASVs that were of common importance for both random forest models.

nonremission state before antibiotic administration, but at the same time, these samples introduce antibiotic treatment as a confounding factor (Model 2, weeks 0, 4, and 8). Model 2 classified remission in MET patients with improved accuracy and

an AUC of 0.879 (95% CI, 0.683–0.9877; sensitivity, 0.7778; specificity, 1.000;  $P < 0.001$ ) and remission in the MET+AZ group with a lower AUC of 0.695 (95% CI, 0.5038–0.7156; sensitivity, 0.20513; specificity, 0.93878;  $P = 0.1672$ ) (Fig. 5A).

Models 1 and 2 each assigned importance scores to each ASV based on the increase in model prediction error when that feature was randomly permuted while all others were left unchanged. The 10 most important ASVs in each model are displayed in Fig. 5B. The most important ASV for both models was ASV 291 (*Lactobacillus*) (Fig. 5B). The ASVs with high importance scores had different abundances in pre-antibiotics, remission, and nonremission samples. Compared with their relative abundances in pre-antibiotic samples, we observed a large increase in ASV 291 (*Lactobacillus*), ASV 60 (*Klebsiella*), and ASVs 2 and 154 (both *Bifidobacterium*), specifically in remission samples (Fig. 5C). In agreement with the results shown in Figure 3, we observed an increase in the abundance of ASVs 7 and 61 (both *Enterococcus*) from the pre-antibiotic state, but no difference between remission and nonremission samples. ASVs that decreased in remission samples but not in nonremission samples included ASV 16 (*Fusicatenibacter saccharivorans*) and ASV 24 (*Dorea longicatena*).

We wondered whether there were microbial signatures present before antibiotic administration that would predict remission after treatment. Although not statistically significant, pre-antibiotic samples from MET subjects who were in remission at week 4 trended toward higher alpha diversity (Supplementary Fig. 4A), a pattern reported in other prediction-focused studies.<sup>27, 28</sup> Due to the limited number of pre-antibiotic samples available, we combined samples from both treatment groups and information on each subject's age, sex, disease duration, tissue involvement, and the current disease state. Unfortunately, we still were not able to construct a robust model (AUC, 0.8; 95% CI, 0.4099–0.8666; sensitivity, 0.8; specificity, 0.5;  $P = 0.24$ ) (Supplementary Fig. 4B). However, we identified ASV clusters with higher mean abundance in pre-antibiotic samples of subjects who went on to achieve remission, such as Cluster 8 (*Peptostreptococcaceae*), Cluster 24 (*Alistipes*), Cluster 23 (*Clostridium sensu stricto*), and Cluster 27 (*Parabacteroides*) (Supplementary Fig. 4C). In contrast, for example, ASV Cluster 61 (*Fusobacterium*) was more abundant in pre-antibiotic samples of subjects who did not subsequently achieve remission, in accordance with other studies.<sup>7–9</sup>

## DISCUSSION

In this study, we determined the effects of MET-only and combination MET+AZ therapy on the gut microbiota in pediatric CD patients. We demonstrated a treatment-specific effect of both antibiotic regimens on microbiota structure, especially at the time of clinical disease remission. We assessed the utility of microbiota signatures for classifying disease remission and the capacity of the baseline (pre-antibiotic) microbiota structure to predict future treatment response.

In comparison with previous work, the strength of our study lies in the use of samples from a multinational cohort and from CD patients exclusively. Small cohort size is a common problem and has led to co-evaluation of samples from mixed

patient populations with CD and ulcerative colitis, whereas recent data have highlighted the differences between those subtypes of IBD with respect to the microbiota.<sup>29</sup> Second, many previous studies have characterized the microbiota of patients based on 1 sample and time point,<sup>7, 9</sup> whereas the design of this study provided an opportunity to monitor the microbiota before, during, and after treatment, which we believe is critical for identifying microbial signatures related to different clinical outcomes.

We acknowledge weaknesses in the study design, such as failed randomization of sex and subjects with L1 Paris classification and observed impact of 5ASA on the baseline microbiome, although the distribution of 5ASA between treatment groups was equal. The use of additional medication by some patients during the study was also a potential confounding factor. The switching between treatment arms upon failure to achieve remission also complicated our analysis. These factors are difficult to navigate in a patient population with such a complex disease and individual treatment requirements. Furthermore, our ability to build a robust predictive model for both treatment arms was limited by the sample size.

It is well established that antibiotic treatment creates an ecosystem-wide disturbance and decreases the overall diversity of the gut microbiome.<sup>30</sup> To our knowledge, few studies have examined the effects of single vs combination antibiotics on the gut microbiome.<sup>31</sup> Although we observed a general decrease in diversity in response to antibiotics, our results also showed a distinct impact on microbiota structure and a shift in abundance of specific bacterial ASVs in each treatment group. These findings highlight the need to understand better the additive, antagonistic, synergistic, and nonlinear effects of antibiotic treatments with regards to patient outcome. Despite different effects on the gut microbiota, the 2 treatments both produced remission-compatible microbiota configurations.

Metronidazole is one of the most prescribed antibiotics in the treatment of pediatric CD, but to our knowledge, there has been no in-depth study of the effects of metronidazole treatment on the gut microbiota in humans to date. One study in mice, comparing the impact of metronidazole vs streptomycin on the microbiota and subsequent *Citrobacter rodentium*-induced colitis, observed treatment-specific effects not only on microbiota structure but also on gut mucosal immune responses.<sup>32</sup> In the absence of *C. rodentium* infection, metronidazole was found to decrease goblet cell expression of MUC2, thereby leading to a thinning of the inner mucus layer, which could be detrimental for intestinal homeostasis and promote chronic intestinal inflammation. Although this observation has not been confirmed in humans, it has important implications for the use of MET in IBD patients.

Recent studies reported superior outcomes for MET plus AZ, as compared with MET alone.<sup>13, 14</sup> AZ penetrates multiple intestinal compartments<sup>15, 16</sup> and enables targeting of adherent and invasive *E. coli* (AIEC) strains and other bacteria

that have been associated with CD at disease onset in children.<sup>9, 17–19</sup> Consistent with previous reports, we observed reduced abundances of ASV 4 (*Escherichia/Shigella*) in the MET+AZ group but increased abundances in the MET group, which may reflect activity of azithromycin against this taxon in our cohort. To assess the presence of AIEC specifically, patient biopsies could be used in the future to access the mucosa-adherent or intracellular microbial constituents.

We also observed that some bacterial taxa such as *Enterococcus*, *Streptococcus*, *Klebsiella*, *Bifidobacterium*, and *Enterobacteriaceae* increased in abundance during antibiotic treatment. This could be due to creation or expansion of nutritional and/or environmental niches during or after general community disturbance, or it could indicate intrinsic or acquired antibiotic resistance. Our finding of increased abundances of *Enterococcus* ASVs in both treatment groups is concerning, as they possess multiple mechanisms for resisting antibiotics; their expansion could predispose patients to invasive infections.<sup>33, 34</sup>

An important question is whether the microbiome itself might be used as a therapeutic agent for Crohn's disease, for example, by administration of specific beneficial microbes as probiotics.<sup>35</sup> Our study identified multiple *Lactobacillus* ASVs that were important for the classification of clinical remission and whose abundance significantly increased during remission. *Lactobacillus* species are commonly used as probiotics, and several in vitro and animal studies have suggested that they may reduce inflammation in CD.<sup>36, 37</sup> In humans, clinical trials with *Lactobacillus* probiotics in CD patients have so far been unsuccessful,<sup>38, 39</sup> highlighting the need to understand not only the biology of *Lactobacillus* species but microbial community ecology.

Two recent studies used microbiota data to predict the success of biologics in adult IBD patients and identified taxa associated with disease remission. Ananthakrishnan et al. reported a decrease in abundance of 5 taxa associated with remission in response to anti-integrin biologic therapy—among them *Bifidobacterium longum*.<sup>40</sup> In contrast, we observed a large increase in abundance of 2 *Bifidobacterium* ASVs in antibiotic-associated remission samples. Doherty et al. showed that the relative abundance of *Escherichia/Shigella* was lower in subjects in remission associated with ustekinumab therapy than it was in subjects with active CD.<sup>27</sup> In our study subjects, we observed decreased abundance of an *Escherichia/Shigella* ASV in the MET+AZ group, which achieved higher remission rates, although the ASV was not implicated in our predictive model of remission. Both studies reported higher microbiota alpha diversity at baseline in patients who later achieved remission. Although not statistically significant, baseline samples from MET subjects in our cohort who achieved remission at week 4 trended toward higher alpha diversity as well.

We suggest that random forest models can be useful for microbiota-based classification and prediction. Our efforts in constructing useful classifiers for disease remission or

prediction of treatment response to antibiotics draw attention to the importance and difficulties of obtaining sufficient numbers of subjects and samples. Moreover, the identification of remission-associated patterns may depend on the cohort characteristics, such as age and disease duration, and on the therapy, its dosage, and duration.

## CONCLUSIONS

There are several important implications of our findings. Our results suggest that there is no single antibiotic-associated remission state, but that different regimens may impact the microbiome in a distinct manner yet lead to remission. We show that the classification of pediatric CD patients in antibiotic-associated clinical remission based on their microbiota structure is possible, although large sample sizes will be required for accurate model construction. We suggest that classification and prediction models based on microbiota signatures may be another tool for monitoring disease and treatment response. Moreover, such models may also assist in the development and testing of more precise approaches for microbiome manipulation and might eventually lead to more effective management of CD and other forms of inflammatory bowel disease.

## SUPPLEMENTARY DATA

Supplementary data are available at *Inflammatory Bowel Diseases* online.

## ACKNOWLEDGMENTS

We are grateful to the study participants. We thank Alvaro Hernandez at the University of Illinois Roy J. Carver Biotechnology Center for outstanding DNA sequencing services.

## REFERENCES

1. Benchimol EI, Fortinsky KJ, Gozdyra P, et al. Epidemiology of pediatric inflammatory bowel disease: a systematic review of international trends. *Inflamm Bowel Dis*. 2011;17:423–439.
2. Van Limbergen J, Russell RK, Drummond HE, et al. Definition of phenotypic characteristics of childhood-onset inflammatory bowel disease. *Gastroenterology*. 2008;135:1114–1122.
3. Heuschkel R, Salvestrini C, Beattie RM, et al. Guidelines for the management of growth failure in childhood inflammatory bowel disease. *Inflamm Bowel Dis*. 2008;14:839–849.
4. Lichtenstein GR, McGovern DPB. Using markers in IBD to predict disease and treatment outcomes: rationale and a review of current status. *Am J Gastroenterol Suppl*. 2016;3:17–26.
5. Soubières AA. Emerging role of novel biomarkers in the diagnosis of inflammatory bowel disease. *World J Gastrointest Pharmacol Ther*. 2016;7:41–50.
6. Khor B, Gardet A, Xavier RJ. Genetics and pathogenesis of inflammatory bowel disease. *Nature*. 2011;474:307–317.
7. Papa E, Docktor M, Smillie C, et al. Non-invasive mapping of the gastrointestinal microbiota identifies children with inflammatory bowel disease. *PLoS One*. 2012;7:e39242.
8. Shaw KA, Bertha M, Hofmekler T, et al. Dysbiosis, inflammation, and response to treatment: a longitudinal study of pediatric subjects with newly diagnosed inflammatory bowel disease. *Genome Med*. 2016;8:75.
9. Gevers D, Kugathasan S, Denson LA, et al. The treatment-naïve microbiome in new-onset Crohn's disease. *Cell Host Microbe*. 2014;15:382–392.
10. Manichanh C, Rigottier-Gois L, Bonnaud E, et al. Reduced diversity of faecal microbiota in Crohn's disease revealed by a metagenomic approach. *Gut*. 2006;55:205–211.

11. Dethlefsen L, Huse S, Sogin ML, et al. The pervasive effects of an antibiotic on the human gut microbiota, as revealed by deep 16S rRNA sequencing. *PLoS Biol.* 2008;6:e280.
12. Scribano ML, Prantero C. Use of antibiotics in the treatment of Crohn's disease. *World J Gastroenterol.* 2013;19:648–653.
13. Levine A, Kori M, Kierkus J, et al. Azithromycin and metronidazole versus metronidazole-based therapy for the induction of remission in mild to moderate paediatric Crohn's disease: a randomised controlled trial. *Gut.* 2019;68:239–247.
14. Levine A, Turner D. Combined azithromycin and metronidazole therapy is effective in inducing remission in pediatric Crohn's disease. *J Crohns Colitis.* 2011;5:222–226.
15. Høiby N, Bjarnsholt T, Givskov M, et al. Antibiotic resistance of bacterial biofilms. *Int J Antimicrob Agents.* 2010;35:322–332.
16. Lutz L, Pereira DC, Paiva RM, et al. Macrolides decrease the minimal inhibitory concentration of anti-pseudomonas agents against pseudomonas aeruginosa from cystic fibrosis patients in biofilm. *BMC Microbiol.* 2012;12:196.
17. Glasser AL, Boudeau J, Barnich N, et al. Adherent invasive *Escherichia coli* strains from patients with Crohn's disease survive and replicate within macrophages without inducing host cell death. *Infect Immun.* 2001;69:5529–5537.
18. Martinez-Medina M, Naves P, Blanco J, et al. Biofilm formation as a novel phenotypic feature of adherent-invasive *Escherichia coli* (AIEC). *BMC Microbiol.* 2009;9:202.
19. Darfeuille-Michaud A, Boudeau J, Bulois P, et al. High prevalence of adherent-invasive *Escherichia coli* associated with ileal mucosa in Crohn's disease. *Gastroenterology.* 2004;127:412–421.
20. Caporaso JG, Kuczynski J, Stombaugh J, et al. QIIME allows analysis of high-throughput community sequencing data. *Nat Methods.* 2010;7:335–336.
21. Callahan BJ, McMurdie PJ, Rosen MJ, et al. DADA2: high-resolution sample inference from Illumina amplicon data. *Nat Methods.* 2016;13:581–583.
22. McMurdie PJ, Holmes S. Phyloseq: an R package for reproducible interactive analysis and graphics of microbiome census data. *PLoS One.* 2013;8:e61217.
23. Levine A, Griffiths A, Markowitz J, et al. Pediatric modification of the Montreal classification for inflammatory bowel disease: the Paris classification. *Inflamm Bowel Dis.* 2011;17:1314–1321.
24. Dethlefsen L, Relman DA. Incomplete recovery and individualized responses of the human distal gut microbiota to repeated antibiotic perturbation. *Proc Natl Acad Sci USA.* 2011;108(Suppl 1):4554–4561.
25. Lozupone C, Knight R. Unifrac: a new phylogenetic method for comparing microbial communities. *Appl Environ Microbiol.* 2005;71:8228–8235.
26. Retsema JA, Girard AE, Girard D, et al. Relationship of high tissue concentrations of azithromycin to bactericidal activity and efficacy in vivo. *J Antimicrob Chemother.* 1990;25(Suppl A):83–89.
27. Doherty MK, Ding T, Koumpouras C, et al. Fecal microbiota signatures are associated with response to ustekinumab therapy among Crohn's disease patients. *MBio.* 2018;9:02120–17.
28. Zhou Y, Xu ZZ, He Y, et al. Gut microbiota offers universal biomarkers across ethnicity in inflammatory bowel disease diagnosis and infliximab response prediction. Ercolini D, ed. *mSystems.* 2018;3:1063–1014.
29. Pascal V, Pozuelo M, Borruel N, et al. A microbial signature for Crohn's disease. *Gut.* 2017;66:813–822.
30. Sullivan A, Edlund C, Nord CE. Effect of antimicrobial agents on the ecological balance of human microflora. *Lancet Infect Dis.* 2001;1:101–114.
31. Weber D, Hiergeist A, Weber M, et al. Detrimental effect of broad-spectrum antibiotics on intestinal microbiome diversity in patients after allogeneic stem cell transplantation: lack of commensal sparing antibiotics. *Clin Infect Dis.* 2019;68:1303–1310.
32. Wlodarska M, Willing B, Keeney KM, et al. Antibiotic treatment alters the colonic mucus layer and predisposes the host to exacerbated citrobacter rodentium-induced colitis. Bäuml AJ, ed. *Infect Immun.* 2011;79:1536–1545.
33. Miller WR, Munita JM, Arias CA. Mechanisms of antibiotic resistance in enterococci. *Expert Rev Anti Infect Ther.* 2014;12:1221–1236.
34. Lebreton F, van Schaik W, Manson McGuire A, et al. Emergence of epidemic multidrug-resistant *Enterococcus faecium* from animal and commensal strains. *MBio.* 2013;4:e00534–13.
35. Ghosh S, van Heel D, Playford RJ. Probiotics in inflammatory bowel disease: is it all gut flora modulation? *Gut.* 2004;53:620–622.
36. Dieleman LA, Goerres MS, Arends A, et al. *Lactobacillus* GG prevents recurrence of colitis in HLA-B27 transgenic rats after antibiotic treatment. *Gut.* 2003;52:370–376.
37. Borruel N, Carol M, Casellas F, et al. Increased mucosal tumour necrosis factor alpha production in Crohn's disease can be downregulated ex vivo by probiotic bacteria. *Gut.* 2002;51:659–664.
38. Prantero C, Scribano ML, Falasco G, et al. Ineffectiveness of probiotics in preventing recurrence after curative resection for Crohn's disease: a randomised controlled trial with *Lactobacillus* GG. *Gut.* 2002;51:405–409.
39. Marteau P, Lémann M, Seksik P, et al. Ineffectiveness of *Lactobacillus johnsonii* LA1 for prophylaxis of postoperative recurrence in Crohn's disease: a randomised, double blind, placebo controlled GETAID trial. *Gut.* 2006;55:842–847.
40. Ananthakrishnan AN, Luo C, Yajnik V, et al. Gut microbiome function predicts response to anti-integrin biologic therapy in inflammatory bowel diseases. *Cell Host Microbe.* 2017;21:603–610.e3.